

# Topotactic hydrogen in nickelate superconductors and akin infinite-layer oxides $ABO_2$

Liang Si,<sup>1,2</sup> Wen Xiao,<sup>1</sup> Josef Kaufmann,<sup>2</sup> Jan M. Tomczak,<sup>2</sup> Yi Lu,<sup>3</sup> Zhicheng Zhong,<sup>1,\*</sup> and Karsten Held<sup>2</sup>

<sup>1</sup>Key Laboratory of Magnetic Materials and Devices & Zhejiang Province  
Key Laboratory of Magnetic Materials and Application Technology,  
Ningbo Institute of Materials Technology and Engineering (NIMTE),  
Chinese Academy of Sciences, Ningbo 315201, China

<sup>2</sup>Institute for Solid State Physics, Vienna University of Technology, 1040 Vienna, Austria

<sup>3</sup>Institute for Theoretical Physics, Heidelberg University, Philosophenweg 19, 69120 Heidelberg, Germany

(Dated: June 7, 2022)

Superconducting nickelates appear to be difficult to synthesize. Since the chemical reduction of  $ABO_3$  ( $A$ : rare earth;  $B$  transition metal) with  $CaH_2$  may result in both,  $ABO_2$  and  $ABO_2H$ , we calculate the topotactic H binding energy by density functional theory (DFT). We find intercalating H to be energetically favorable for  $LaNiO_2$  but not for Sr-doped  $NdNiO_2$ . This has dramatic consequences for the electronic structure as determined by DFT+dynamical mean field theory: that of  $3d^9$   $LaNiO_2$  is similar to (doped) cuprates,  $3d^8$   $LaNiO_2H$  is a two-orbital Mott insulator. Topotactic H might hence explain why some nickelates are superconducting and others are not.

Most recently superconductivity was found in  $Nd_{0.8}Sr_{0.2}NiO_2$  films grown on  $SrTiO_3$  [1], a seminal work that opens the door wide to a new age of superconductivity: the nickelate age. These novel (Sr-doped)  $NdNiO_2$  superconductors are not only isostructural to the well known cuprate superconductor  $CaCuO_2$  [2] but also both, Ni and Cu, are formally  $3d^9$  in the respective parent compound.

Strikingly different to the cuprates [3] and iron pnictides [4], reproducing these outstanding results in iso-electronic compositions appears to be quite challenging. In a more bulk-like crystal, no superconductivity was reported for  $Nd_{0.8}Sr_{0.2}NiO_2$  [5]; neither is  $NdNiO_2$  superconducting [1] but shows a resistivity upturn toward low temperatures. Another nickelate,  $LaNiO_2$ , is also isostructural and isovalent, but is a (bad) metal [6] with no superconductivity nor antiferromagnetism [7].

An obvious difference between  $Nd_{0.8}Sr_{0.2}NiO_2$  and  $Nd(La)NiO_2$  is doping. However, in contrast to the cuprates, there is already a self-doping of the Ni-bands in  $Nd(La)NiO_2$  because one Nd(La) band crosses the Fermi energy [8–11], hardly hybridizing with the Ni- $3d_{x^2-y^2}$  bands. Why are some of these nickelates, all of which have a similar DFT electronic structure in the paramagnetic phase [8–10, 12–15][16], superconducting but others are not?

Let us take a step back and recapitulate the synthesis of  $ANiO_2$  nickelates with the unusual low oxidation state  $Ni^{+}$ . It is synthesized by first growing  $ANiO_3$  on a  $SrTiO_3$  substrate, and then reducing it to  $ANiO_2$  with the help of the reagent  $CaH_2$ , see Fig. 1. However, there is another possible endproduct:  $ANiO_2H$ . Indeed for another perovskite,  $SrVO_3$ , it was shown in a detailed experimental analysis [17] that the  $CaH_2$  reduction reaction leads to  $SrVO_2H$ ; also  $NdNiO_xH_y$  has been detected [18].

In this letter, we show based on DFT calculations [19–21] that the nickelates are just at the borderline of the two reaction paths of Fig. 1: While for  $A=Nd$  and in

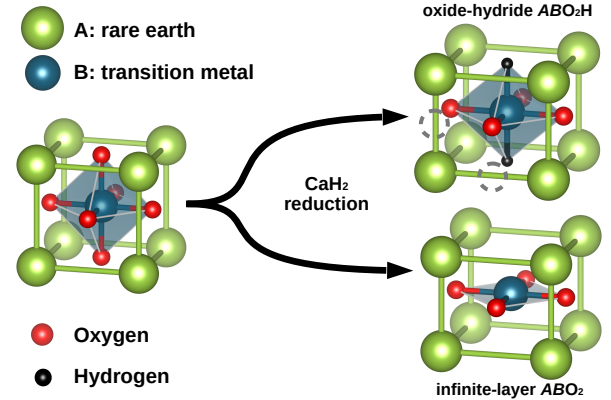


FIG. 1. Two possible products in the topotactic reduction of  $ABO_3$  by means of  $CaH_2$ : oxide-hydrate  $ABO_2H$  and infinite-layer  $ABO_2$ .

particular for  $A=La$  the oxide-hydrates  $NdNiO_2H$  and  $LaNiO_2H$  are energetically favorable, with Sr-doping, the infinite-layer  $Nd_{0.8}Sr_{0.2}NiO_2$  becomes more stable. As a matter of course, the reaction kinetics also influences the endproducts, and without carefully optimizing the reaction conditions some mixed phase of  $ANiO_2$  and  $ANiO_2H$  may emerge. We further demonstrate that the H intercalation has dramatic consequences for the electronic structure as calculated by DFT and DFT+dynamical mean field theory (DMFT) [22–25]: While  $ANiO_2$  is metallic with a very strong quasiparticle renormalization of the Ni  $d_{x^2-y^2}$  band and Nd(La)- $5d$  pocket, quite similar to doped cuprates;  $ANiO_2H$  is a Mott insulator with two Ni bands,  $d_{x^2-y^2}$  and  $d_{z^2}$ , and no Nd(La)- $5d$  pocket.

*Methods.* Structural details and H-topotactic binding energies are computed by DFT structural relaxations and total energy calculations. Both WIEN2K [26] and VASP [27] codes within PBE [28] and PBEsol [29] versions of the generalized gradient approximation (GGA) are employed on a  $13 \times 13 \times 15$  momentum grid.

For the DMFT calculations, the WIEN2K bandstructure around the Fermi level is projected onto Wannier functions [30, 31] using WIEN2WANNIER [32, 33] and supplemented by a local density-density interaction, taking the fully localized limit [34] as double counting. Since for infinite-layer  $\text{LaNiO}_2$ , one  $\text{La-}d$  band crosses the Fermi level  $E_f$ , here a full set of  $\text{La-}5d+\text{Ni-}3d$  bands is adopted. For  $\text{LaNiO}_2\text{H}$ , a projection onto the  $\text{Ni-}3d$  bands is possible only because now the  $\text{La-}5d$  bands are well separated from the  $\text{Ni-}3d$  bands. The interaction parameters are computed by constrained random phase approximation (cRPA) [35]: average inter-orbital interaction  $U' = 3.10$  eV (2.00 eV) and Hund's exchange  $J = 0.65$  eV (0.25 eV) for Ni (La). The intra-orbital Hubbard interaction follows as  $U = U' + 2J$ . These interaction parameters are close to those of previous studies [36, 37] for  $3d$  oxides. The resulting Hamiltonian is then solved at room temperature (300 K) in DMFT using continuous-time quantum Monte Carlo simulations in the hybridization expansions [38] implemented in w2DYNAMIC [39, 40]; the maximum entropy method [41, 42] is employed for an analytic continuation of the spectra.

*Energetics of Topotactic Hydrogen.* Besides the two cornerstone endproducts, infinite-layer  $\text{ABO}_2$  (e.g.,  $\text{CaCuO}_2$ ,  $\text{SrCuO}_2$ ) and oxide-hydride  $\text{ABO}_2\text{H}$  (e.g.,  $\text{SrVO}_2\text{H}$ ), of Fig. 1, also intermediate products such as  $(\text{Ba}, \text{Sr}, \text{Ca})\text{TiO}_{3-x}\text{H}_x$  [43, 44] and  $\text{NdNiO}_x\text{H}_y$  [18] have been experimentally confirmed when reducing  $\text{ABO}_3$  with  $\text{CaH}_2$  upon heating [45]. To investigate whether it is energetically favorable to intercalate hydrogen in the topotactic reaction or not, we compute the hydrogen binding energy

$$E_B = E[\text{ABO}_2] + \mu[\text{H}] - E[\text{ABO}_2\text{H}]. \quad (1)$$

Here,  $E[\text{ABO}_2]$  and  $E[\text{ABO}_2\text{H}]$  are the total energy of  $\text{ABO}_2$  and  $\text{ABO}_2\text{H}$ ; and  $\mu[\text{H}] = E[\text{H}_2]/2$  is the chemical potential of H. Note that  $\text{H}_2$  is a typical byproduct for the reduction with  $\text{CaH}_2$  and also emerges when  $\text{CaH}_2$  is in contact with  $\text{H}_2\text{O}$ . Hence it can be expected to be present in the reaction.  $E_B$  is also the difference in binding energy for the two reaction paths of Fig. 1, i.e., it is energetically favorable by  $E_B$  to synthesize  $\text{ABO}_2\text{H}$  instead of  $\text{ABO}_2$  and  $\text{H}_2/2$ . Of course the reaction kinetics may change the outcome and the large entropy of  $1/2 \text{H}_2$  might change the balance thermodynamically in favor of  $\text{ABO}_2$  [46]. But at the very least the energetics gives us a first hint whether to expect  $\text{ABO}_2\text{H}$  or  $\text{ABO}_2$ .

As for the three H-positions of Fig. 1, we always find that the vacancy left by the removed oxygen is the energetically favored H-position. For a full H-topotactic intercalation, i.e.,  $\text{ABO}_2\text{H}$  with all vacant oxygen positions occupied by H, this is plotted explicitly in Fig. 1. We first consider this complete intercalation, fully relax the  $\text{ABO}_2$  and  $\text{ABO}_2\text{H}$  structures, and then calculate the respective total paramagnetic DFT energy and from this  $E_B$  through Eq. (1). For  $\text{SrBO}_2$  and  $\text{LaBO}_2$ ,  $E_B$

is positive from Ti to Co in Fig. 2(a), indicating the energetical preference for the oxide-hydride  $\text{SrBO}_2\text{H}$  for  $B=\text{Ti}\dots\text{Co}$ . This is consistent with finding  $\text{SrVO}_2\text{H}$  and  $\text{SrTiO}_x\text{H}_y$  after  $\text{CaH}_2$  reduction [17, 47–49]. Similarly, oxide-hydrides have been reported experimentally when reducing  $(\text{Sr}, \text{La})\text{CoO}_3$  [50, 51] and  $(\text{Ba}, \text{Ca}, \text{Sr})\text{TiO}_3$  [44, 52, 53].

Surprisingly, for  $\text{LaNiO}_2$ , a positive  $E_B$  of 0.162 eV is predicted, too. This indicates incorporating H topotactically in infinite-layer  $\text{LaNiO}_2$  is at least energetically favorable. For  $\text{SrNiO}_2$  on the other hand it is energetically unfavorable to intercalate H. That is, the nickelates  $\text{ANiO}_2$  are just at the border line  $E_B = 0$  in Fig. 2(a); the cation  $A$  is decisive. The cuprates on the other hand are clearly on the  $E_B < 0$  side, i.e., hydrogen will not be intercalated, consistent with the well studied chemistry of the cuprates.

Besides the La- and Sr-based infinite-layer  $\text{ABO}_2$ , we also calculate  $E_B$  for a few additional materials:  $\text{CaCuO}_2$  [2] has  $E_B < 0$  as the other cuprate superconductors; undoped  $\text{NdNiO}_2$  [54] has  $E_B = 0.133$  eV, which turns negative to  $E_B = -0.113$  eV if 25% of Nd atoms are replaced by Sr. Hence our results indicate that infinite-layer, superconducting Sr-doped  $\text{NdNiO}_2$  is energetically stable against the topotactic inclusion of H, whereas other nickelates are not.

The complete (full) topotactic inclusion of H, where all vacancies induced by removing-oxygen are filled by H, is an ideal limiting case. Under varying experimental conditions such as chemical reagent, substrate, temperature and strain, the H-topotactic inclusion may be incomplete, and  $\text{ABO}_2\text{H}_y$  ( $y < 1$ ) energetically favored. Hence we also compute  $E_B$  at a rather low H-topotactic density:  $\text{ABO}_2\text{H}_{0.125}$  (achieved by including a single H into  $2 \times 2 \times 2$   $\text{ABO}_2$  supercells). Additionally, we model strain effects by changing the in-plane lattice constants ( $a$ ,  $b$ ), relaxing the lattice in  $z$ -direction and the internal atomic positions.

Fig. 2(b) shows the corresponding  $E_B$  for  $\text{SrVO}_2\text{H}_{0.125}$ ,  $\text{LaNiO}_2\text{H}_{0.125}$ , and  $\text{CaCuO}_2\text{H}_{0.125}$ . Unstrained (0%), the binding energy  $E_B$  per hydrogen (0.620 eV for  $\text{SrVO}_2\text{H}_{0.125}$ , 0.094 eV for  $\text{LaNiO}_2\text{H}_{0.125}$  and -0.945 eV for  $\text{CaCuO}_2\text{H}_{0.125}$ ) is very similar to complete hydrogen intercalation ( $E_B = 0.637$  eV for  $\text{SrVO}_2\text{H}$ , 0.162 eV for  $\text{LaNiO}_2\text{H}$  and -0.859 eV for  $\text{CaCuO}_2\text{H}$ ) in Fig. 2(a). This indicates that the topotactic intercalation with H is essentially independent of the hydrogen density. Fig. 2(b) further shows that  $E_B$  is substantially reduced by compressive (negative) strain. This is because the compressive strain enlarges the  $z$ -axis, which in turn leads to weaker H-B-H bonding. This suggests compression to be an effective way to eliminate residual H in  $\text{ANiO}_2$ . It might also explain why  $\text{NdNiO}_2$  was found next to the interface of (compressive)  $\text{SrTiO}_3$ , whereas  $\text{NdNiO}_x\text{H}_y$  was found further away from the interface [18].

Let us now ask: Why is  $E_B$  varying remarkably for

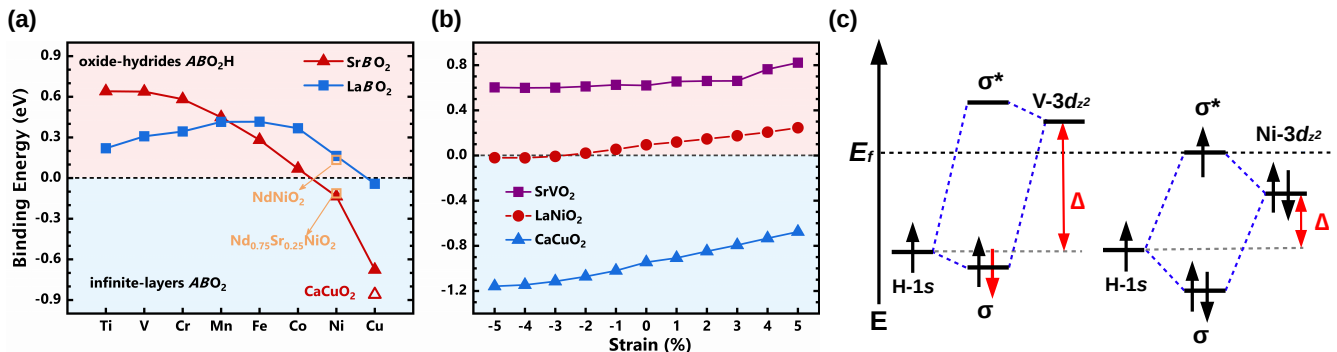


FIG. 2. (a) Binding energy  $E_B$  for topotactic H in infinite-layer  $ABO_2$  ( $A$ : Sr or La;  $B$ : Ti to Cu). Further,  $E_B$  for  $CaCuO_2$ ,  $NdNiO_2$  and  $Nd_{0.75}Sr_{0.25}NiO_2$  is plotted. (b)  $E_B$  for  $SrVO_2$ ,  $LaNiO_2$  and  $CaCuO_2$  as a function of strain, at a low H-density of 12.5%. (c) Explanation of the evolution of the H-topotactic binding energy from  $AVO_2$  to  $ANiO_2$  based on the formation of bonding ( $\sigma$ ) and anti-bonding ( $\sigma^*$ ) states between H-1s and transition metal  $3d_{z^2}$ . The up/down arrows indicate the electron spins, the red arrow for  $AVO_2$  means the electron is from other ( $V-t_{2g}$ ) orbitals.

different  $ABO_2$ ? Besides the gradually changing lattice constants, the dominating factor is the  $d$ -band filling. By computing the band characteristics (Fig. 3 below), we find  $H^-$  which, similar to  $O_{0.5}^{2-}$ , absorbs one Ni electron. For early transition metals with positive  $E_B$ , as e.g.  $SrVO_2H$ , the H-1s forms bonding ( $\sigma$ ) and anti-bonding ( $\sigma^*$ ) states due to the orbital overlap with  $V-d_{z^2}$  as sketched in the left panel of Fig. 2(c). The bonding  $\sigma$  orbital is fully occupied with one electron originating for the H-1s and the second from the  $V-t_{2g}$  orbitals. This explains the stabilization and energy gain of  $SrVO_2H$ .

For late transition metals, e.g.  $LaNiO_2H$ , the  $3d_{z^2}$  is fully filled, see right panel of Fig. 2(c). Hence, when intercalating H also the anti-bonding  $\sigma^*$  orbital needs to be occupied with one electron and then crosses  $E_F$ . This and the smaller bonding-antibonding splitting reduces the energy gain for the topotactic intercalation of H. This puts the nickelates at the borderline, whereas for the next transition metal, Cu, it is no longer energetically favorable to form  $ACuO_2H$ .

*DFT Electronic structure.* Let us now address the question: How much does the electronic structure change if topotactic hydrogen is present? In the infinite-layer  $LaNiO_2$  the Ni  $d_{x^2-y^2}$  orbital shows a single-band dispersion without hybridization with other bands, similar to the Cu- $d_{x^2-y^2}$  dispersion in cuprates. However, in contrast to the cuprates there is an itinerant La-band which crosses  $E_f$  around the  $A$ -point, see Fig. 3(a) and [9–12]. It is composed of of La-5d but also La-4f and with some Ni- $t_{2g}$  intermixing. There is no discernible hybridization gap when this La-band crosses the Ni- $d_{x^2-y^2}$  band in Fig. 3(a), because of the (symmetry-dictated) very weak hybridization between both [11].

For  $LaNiO_2H$ , the topotactic H alters the DFT band structure completely, see Fig. 3(b). Firstly, the La band-crossing at  $E_F$  around the  $A$ -point is gone. This is because the La- $d_{xy}$  hopping in the (110) direction changes

sign when connected through the H-1s orbital: from  $-0.098$  eV for  $LaNiO_2$  to  $0.224$  eV for  $LaNiO_2H$ . This turns the minimum (La-5d pocket) around the  $A$ -point in Fig. 3(a) into a maximum in Fig. 3(b). Secondly, the Ni- $d_{z^2}$  band is now partially occupied for  $LaNiO_2H$  instead of being fully occupied in infinite-layer  $LaNiO_2$ . Three factors contribute to this: (1) The local Ni- $d_{z^2}$  potential is shifted up by  $\sim 1.5$  eV because the  $d_{z^2}$  orbitals point towards the negatively charged  $H^-$ . (2) The intra-orbital, nearest-neighbor hopping of the  $d_{z^2}$  electrons along  $k_z$  [ $\Gamma$  to  $Z$  in Fig. 3 (a,b)] changes sign from  $-0.308$  eV for  $LaNiO_2$  to  $0.781$  eV for  $LaNiO_2H$ . (3) Last but not least,  $H^-$  reduces the valence of Ni from  $Ni^{9+}$  to  $Ni^{8+}$ , effectively reducing  $E_f$ . Altogether, we end up in a situation which is much less akin to the cuprates: a  $3d^8$  electronic configuration with two Ni orbitals,  $3d_{x^2-y^2}$  and  $d_{z^2}$ , but no La-5d band around  $E_F$ .

*DFT+DMFT electronic structure.* Let us now turn to the effects of correlations, which are expected to be strong in such transition metal oxides. To this end we perform DFT+DMFT calculations at room-temperature (300 K) in the paramagnetic phase. For  $LaNiO_2$  [Fig. 4(a)], electronic correlations lead to a dramatic quasiparticle renormalization  $Z$  or mass enhancement  $m^*/m = 1/Z \sim 7$  of the almost half-filled Ni  $3d_{x^2-y^2}$  band, see zoom-in Fig. 4(b); the other Ni- $3d$  bands are almost completely filled and below  $E_F$ . The reason for this strong renormalization, somewhat larger than in the previous DFT+DMFT study [55] using  $NdNiO_3$  lattice constants, is that a half-filled Ni  $3d_{x^2-y^2}$ -band would be Mott insulating. Only through the doping via the La-5d band, metallicity is induced in DMFT. Also in DMFT this La-5d band crosses  $E_F$  around the  $A$ -point, see Fig. 4(a). Actually its band dispersion hardly changes since the La-5d bands are only lightly occupied. One noteworthy effect of electronic correlations is however to reduce the number of holes (vs. half-filling) in

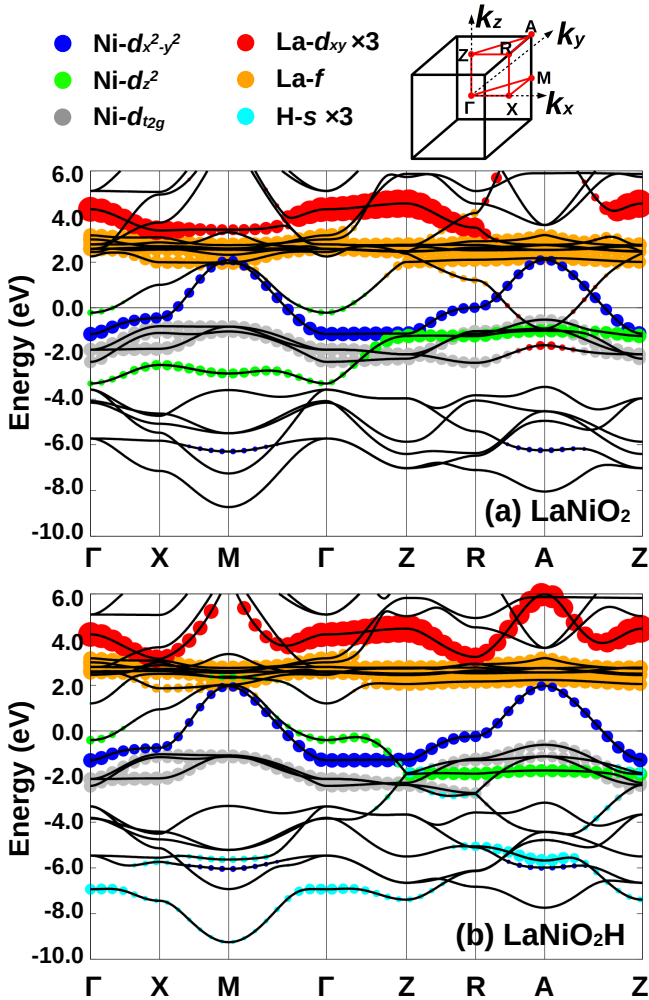


FIG. 3. DFT band structure and orbital characters for (a)  $\text{LaNiO}_2$  and (b)  $\text{LaNiO}_2\text{H}$  along a high symmetry path through the Brillouin zone (top).

the  $3d_{x^2-y^2}$  orbital, from 0.08 per Ni site for the DFT-derived Wannier Hamiltonian to 0.03 in DMFT. Without additional Sr-doping such a light hole doping is likely not enough to induce superconductivity.

For the oxide-hydride  $\text{LaNiO}_2\text{H}$ , on the other hand, the La-5d pockets around the A-point are eliminated not only in DFT [Fig. 3(b)] but also in DFT+DMFT [Fig. 4(c)]. Without doping through the La-5d pocket and the additional  $\text{H}^-$ , Ni is in an undoped  $3d^8$  configuration with holes in both the  $d_{z^2}$ - and  $d_{x^2-y^2}$ -orbitals. This integer filling of the Ni  $d$ -orbitals drives  $\text{LaNiO}_2\text{H}$  into a Mott insulating phase with a gap of  $\sim 0.3$  eV in Fig. 4(c). It is consistent with the experimental observations that  $\text{LaNiO}_{2.5}$ , having formally the same Ni valence, was found to be insulating [56, 57]. While here we find that already the paramagnetic phase is insulating,  $C$ - or  $G$ -type antiferromagnetic ordering [58] can be expected. Similarly  $\text{SrVO}_2\text{H}$  is antiferromagnetic with a high- $T_N$

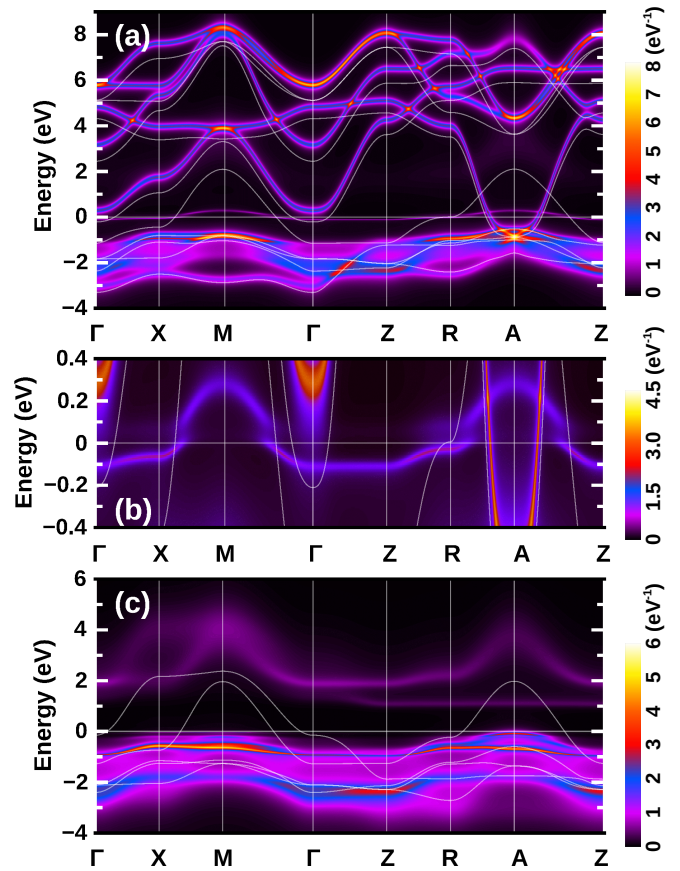


FIG. 4. DMFT spectral functions  $A(k, \omega)$  of (a)  $\text{LaNiO}_2$  and (c)  $\text{LaNiO}_2\text{H}$ ; solid lines: DFT Wannier-bands. Panel (b) is a zoom-in of (a) around  $E_F = 0$ .

[47], whereas  $\text{SrVO}_3$  is a paramagnetic metal.

*Conclusion and outlook.* In another class of correlated superconductors, the iron pnictides [4] [59], it is well known that hydrogen plays an important role [60], also when using  $\text{CaH}_2$  as a reduction reagent [61]. Here, by performing DFT calculations, we find that the topotactic intercalation of hydrogen in infinite-layer  $\text{ABO}_2$  is energetically favorable for early transition metals  $B$ .

This intercalation has dramatic consequences for the electronic structures.  $\text{LaNiO}_2\text{H}$  is a  $3d^8$  Mott insulator with two relevant orbitals around  $E_F$ ,  $3d_{z^2}$  and  $3d_{x^2-y^2}$ , but no La-5d pockets: A situation which is distinctively different from the cuprate superconductors. Indeed this two orbital situation bears some similarities to  $\text{LaNiO}_3/\text{LaAlO}_3$  heterostructures prior to engineering their bandstructure to a cuprate-like one [62–67]. On the other hand,  $\text{LaNiO}_2$  with a  $3d^9$  configuration and the holes only in the  $d_{x^2-y^2}$ -orbital closely resembles the bandstructure of the doped cuprates. This  $d_{x^2-y^2}$ -orbital is doped already for the parent compound because of La-5d pockets, which otherwise do not play a decisive role.

The strikingly different susceptibility toward topotactic intercalation of hydrogen and the dramatic conse-

quences for the electronic structure may explain why some nickelates have been found to be superconducting and others not. Experimentally, one might also expect regions or layers of metallic La(Nd)NiO<sub>2</sub> and insulating La(Nd)NiO<sub>2</sub>H. Such inhomogeneities have already been observed in some experiments [18, 68], and residual side peaks in some x-ray absorption spectra [5, 69] might also indicate secondary phases.

Our findings call for a careful reanalysis of the hydrogen content in nickelates. While hydrogen is difficult to detect, careful studies already confirmed intercalated hydrogen when reducing SrVO<sub>3</sub> [17], SmFeAsO [61], and NdNiO<sub>3</sub> [18] with the reagent CaH<sub>2</sub>. Our calculations further suggest that for synthesizing ANiO<sub>2</sub> without H and an electronic structure prone to superconductivity, compressive strain, Sr-doping and high reaction temperatures are of advantage. Quite a number of capping layers might be needed to stabilize the system against further hydrogen intercalation, and doping with a divalent cation such as Sr appears to be necessary to arrive in the superconductive doping regime.

### Acknowledgments

L. S., W. X. and Z. Z. gratefully acknowledge financial support from the National Key R&D Program of China (2017YFA0303602), 3315 Program of Ningbo, and the National Nature Science Foundation of China (11774360, 11904373). L. S., J. K., J. M. T. and K. H. were supported by the Austrian Science Fund (FWF) through projects P 30997 and P 32044. Y. L. acknowledges support by Deutsche Forschungsgemeinschaft (DFG) under Germanys Excellence Strategy EXC2181/1-390900948 (the Heidelberg STRUCTURES Excellence Cluster). Calculations have been done on the Vienna Scientific Clusters (VSC) and the Supercomputing Center at NIMTE CAS.

---

\* zhong@nimte.ac.cn

- [1] D. Li, K. Lee, B. Y. Wang, M. Osada, S. Crossley, H. R. Lee, Y. Cui, Y. Hikita, and H. Y. Hwang, *Nature* **572**, 624 (2019).
- [2] T. Siegrist, S. Zahurak, D. Murphy, and R. Roth, *nature* **334**, 231 (1988).
- [3] J. G. Bednorz and K. A. Müller, *Zeitschrift für Physik B Condensed Matter* **64**, 189 (1986).
- [4] Y. Kamihara, H. Hiramatsu, M. Hirano, R. Kawamura, H. Yanagi, T. Kamiya, and H. Hosono, *Journal of the American Chemical Society* **128**, 10012 (2006), <https://doi.org/10.1021/ja063355c>.
- [5] Q. Li, C. He, J. Si, X. Zhu, Y. Zhang, and H.-H. Wen, *preprint*, arXiv:1911.02420 (2019).
- [6] D. Kaneko, K. Yamagishi, A. Tsukada, T. Manabe, and M. Naito, *Physica C: Superconductivity* **469**, 936 (2009), proceedings of the 21st International Symposium on Superconductivity (ISS 2008).
- [7] M. A. Hayward, M. A. Green, M. J. Rosseinsky, and J. Sloan, *Journal of the American Chemical Society* **121**, 8843 (1999).
- [8] G.-M. Zhang, Y.-F. Yang, and F.-C. Zhang, *preprint*, arXiv:1909.11845 (2019).
- [9] Y. Nomura, M. Hirayama, T. Tadano, Y. Yoshimoto, K. Nakamura, and R. Arita, *preprint*, arXiv:1909.03942 (2019).
- [10] M. Hirayama, T. Tadano, Y. Nomura, and R. Arita, *preprint*, arXiv:1910.03974 (2019).
- [11] P. Jiang, L. Si, Z. Liao, and Z. Zhong, *arXiv preprint arXiv:1909.13634* (2019).
- [12] K.-W. Lee and W. E. Pickett, *Phys. Rev. B* **70**, 165109 (2004).
- [13] M. Jiang, M. Berciu, and G. A. Sawatzky, *preprint*, arXiv:1909.02557 (2019).
- [14] P. Werner and S. Hoshino, *preprint*, arXiv:1910.00473 (2019).
- [15] H. Sakakibara, H. Usui, K. Suzuki, T. Kotani, H. Aoki, and K. Kuroki, *preprint*, arXiv:1909.00060 (2019).
- [16] One difference is that Nd has a 4f moment and La has not. But because of the weak hybridization with the Ni-3d<sub>x<sup>2</sup>-y<sup>2</sup></sub>, one might expect these to order or undergo a Kondo screening only at prohibitively low temperatures.
- [17] T. Katayama, A. Chikamatsu, K. Yamada, K. Shigematsu, T. Onozuka, M. Minohara, H. Kumigashira, E. Ikenaga, and T. Hasegawa, *Journal of Applied Physics* **120**, 085305 (2016).
- [18] T. Onozuka, A. Chikamatsu, T. Katayama, T. Fukumura, and T. Hasegawa, *Dalton Transactions* **45**, 12114 (2016).
- [19] P. Hohenberg and W. Kohn, *Phys. Rev.* **136**, B864 (1964).
- [20] W. Kohn and L. J. Sham, *Phys. Rev.* **140**, A1133 (1965).
- [21] R. M. Martin, *Electronic Structure: Basic Theory and Practical Methods* (Cambridge University Press Cambridge, 2004).
- [22] A. Georges, G. Kotliar, W. Krauth, and M. J. Rozenberg, *Rev. Mod. Phys.* **68**, 13 (1996).
- [23] G. Kotliar and D. Vollhardt, *Physics Today* **57**, 53 (2004).
- [24] W. Metzner and D. Vollhardt, *Phys. Rev. Lett.* **62**, 324 (1989).
- [25] K. Held, *Advances in physics* **56**, 829 (2007).
- [26] P. Blaha, K. Schwarz, G. Madsen, D. Kvasnicka, and J. Luitz, An augmented plane wave+ local orbitals program for calculating crystal properties (2001).
- [27] G. Kresse and J. Hafner, *Phys. Rev. B* **48**, 13115 (1993).
- [28] J. P. Perdew, K. Burke, and M. Ernzerhof, *Phys. Rev. Lett.* **77**, 3865 (1996).
- [29] J. P. Perdew, A. Ruzsinszky, G. I. Csonka, O. A. Vydrov, G. E. Scuseria, L. A. Constantin, X. Zhou, and K. Burke, *Phys. Rev. Lett.* **100**, 136406 (2008).
- [30] G. H. Wannier, *Phys. Rev.* **52**, 191 (1937).
- [31] N. Marzari, A. A. Mostofi, J. R. Yates, I. Souza, and D. Vanderbilt, *Rev. Mod. Phys.* **84**, 1419 (2012).
- [32] A. A. Mostofi, J. R. Yates, Y.-S. Lee, I. Souza, D. Vanderbilt, and N. Marzari, *Computer physics communications* **178**, 685 (2008).
- [33] J. Kuneš, R. Arita, P. Wissgott, A. Toschi, H. Ikeda, and K. Held, *Computer Physics Communications* **181**, 1888 (2010).

- [34] V. I. Anisimov, J. Zaanen, and O. K. Andersen, *Phys. Rev. B* **44**, 943 (1991).
- [35] T. Miyake and F. Aryasetiawan, *Phys. Rev. B* **77**, 085122 (2008).
- [36] I. A. Nekrasov, K. Held, G. Keller, D. E. Kondakov, T. Pruschke, M. Kollar, O. K. Andersen, V. I. Anisimov, and D. Vollhardt, *Phys. Rev. B* **73**, 155112 (2006).
- [37] G. Lantz, M. Hajlaoui, E. Papalazarou, V. L. R. Jacques, A. Mazzotti, M. Marsi, S. Lupi, M. Amati, L. Gregoratti, L. Si, Z. Zhong, and K. Held, *Phys. Rev. Lett.* **115**, 236802 (2015).
- [38] E. Gull, A. J. Millis, A. I. Lichtenstein, A. N. Rubtsov, M. Troyer, and P. Werner, *Rev. Mod. Phys.* **83**, 349 (2011).
- [39] N. Parragh, A. Toschi, K. Held, and G. Sangiovanni, *Phys. Rev. B* **86**, 155158 (2012).
- [40] M. Wallerberger, A. Hausoel, P. Gunacker, A. Kowalski, N. Parragh, F. Goth, K. Held, and G. Sangiovanni, *Computer Physics Communications* **235**, 388 (2019).
- [41] J. E. Gubernatis, M. Jarrell, R. N. Silver, and D. S. Sivia, *Phys. Rev. B* **44**, 6011 (1991).
- [42] A. W. Sandvik, *Phys. Rev. B* **57**, 10287 (1998).
- [43] T. U. Ito, A. Koda, K. Shimomura, W. Higemoto, T. Matsuzaki, Y. Kobayashi, and H. Kageyama, *Physical Review B* **95**, 020301 (R) (2017).
- [44] T. Yajima, A. Kitada, Y. Kobayashi, T. Sakaguchi, G. Bouilly, S. Kasahara, T. Terashima, M. Takano, and H. Kageyama, *Journal of the American Chemical Society* **134**, 8782 (2012).
- [45] T. Yamamoto and H. Kageyama, *Chemistry letters* **42**, 946 (2013).
- [46] The entropy of  $1/2 H_2$  at 500 K is  $S = 7.5 \cdot 10^{-4} \text{ eV/K}$  [70] corresponding to 0.38 eV. On the other hand, the reduction with  $CaH_2$  might lead to a rather high  $H_2$  pressure; and  $ABO_2H$  has a higher entropy than  $ABO_2$ . Its Mott insulating spin-1 (see below) yields  $S = k_B \ln(3) = 1 \cdot 10^{-4} \text{ eV/K}$  corresponding to 0.05 eV at 500K; a prospective disorder entropy of say  $ABO_2H_{0.5}$  would yield  $S = k_B \ln(2) = 0.6 \cdot 10^{-4} \text{ eV/K}$  or 0.03 eV at 500K.
- [47] F. Denis Romero, A. Leach, J. S. Möller, F. Foronda, S. J. Blundell, and M. A. Hayward, *Angewandte Chemie International Edition* **53**, 7556 (2014).
- [48] M. Amano Patino, D. Zeng, S. J. Blundell, J. E. McGrady, and M. A. Hayward, *Inorganic chemistry* **57**, 2890 (2018).
- [49] T. Yamamoto, D. Zeng, T. Kawakami, V. Arcisauskaite, K. Yata, M. A. Patino, N. Izumo, J. E. McGrady, H. Kageyama, and M. A. Hayward, *Nature communications* **8**, 1217 (2017).
- [50] M. Hayward, E. Cussen, J. Claridge, M. Bieringer, M. Rosseinsky, C. Kiely, S. Blundell, I. Marshall, and F. Pratt, *Science* **295**, 1882 (2002).
- [51] R. M. Helps, N. H. Rees, and M. A. Hayward, *Inorganic chemistry* **49**, 11062 (2010).
- [52] T. Sakaguchi, Y. Kobayashi, T. Yajima, M. Ohkura, C. Tassel, F. Takeiri, S. Mitsuoka, H. Ohkubo, T. Yamamoto, J. e. Kim, *et al.*, *Inorganic chemistry* **51**, 11371 (2012).
- [53] Y. Kobayashi, O. J. Hernandez, T. Sakaguchi, T. Yajima, T. Roinsel, Y. Tsujimoto, M. Morita, Y. Noda, Y. Mogami, A. Kitada, *et al.*, *Nature materials* **11**, 507 (2012).
- [54] For (Sr,Nd)NiO<sub>2</sub>, we perform (antiferro-)magnetic GGA+*U* calculations in VASP instead of the non-magnetic calculations for other ABO<sub>2</sub> systems because (i) NdNiO<sub>3</sub> is experimentally determined to be an antiferromagnetic insulator [1] and (ii) non-magnetic VASP calculations for (Sr,Nd)NiO<sub>2</sub> hardly convergence.
- [55] S. Rye, H. Yoon, T. J. Kim, M. Y. Jeong, and M. J. Han, *preprint*, [arXiv:1909.05824](https://arxiv.org/abs/1909.05824) (2019).
- [56] R. D. Sánchez, M. T. Causa, A. Caneiro, A. Butera, M. Vallet-Regí, M. J. Sayagués, J. González-Calbet, F. García-Sanz, and J. Rivas, *Phys. Rev. B* **54**, 16574 (1996).
- [57] M. Abbate, G. Zampieri, F. Prado, A. Caneiro, J. M. Gonzalez-Calbet, and M. Vallet-Regi, *Physical Review B* **65**, 155101 (2002).
- [58] D. Misra and T. K. Kundu, *The European Physical Journal B* **89**, 4 (2016).
- [59] Let us note that DMFT has been quite helpful for understanding the pnictide physics [71–77].
- [60] S. Iimura, S. Matsuishi, H. Sato, T. Hanna, Y. Muraba, S. W. Kim, J. E. Kim, M. Takata, and H. Hosono, *Nature Comm.* **3**, 943 (2012).
- [61] J. Matsumoto, K. Hanzawa, M. Sasase, S. Haindl, T. Katase, H. Hiramatsu, and H. Hosono, *Phys. Rev. Materials* **3**, 103401 (2019).
- [62] J. Chaloupka and G. Khaliullin, *Phys. Rev. Lett.* **100**, 016404 (2008).
- [63] P. Hansmann, X. Yang, A. Toschi, G. Khaliullin, O. K. Andersen, and K. Held, *Phys. Rev. Lett.* **103**, 016401 (2009).
- [64] P. Hansmann, A. Toschi, X. Yang, O. K. Andersen, and K. Held, *Phys. Rev. B* **82**, 235123 (2010).
- [65] X. Wang, M. J. Han, L. de’ Medici, H. Park, C. A. Marianetti, and A. J. Millis, *Phys. Rev. B* **86**, 195136 (2012).
- [66] A. Subedi, O. E. Peil, and A. Georges, *Phys. Rev. B* **91**, 075128 (2015).
- [67] O. Janson and K. Held, *Phys. Rev. B* **98**, 115118 (2018).
- [68] M. Hayward, M. Green, M. Rosseinsky, and J. Sloan, *Journal of the American Chemical Society* **121**, 8843 (1999).
- [69] M. Hepting, D. Li, C. Jia, H. Lu, E. Paris, Y. Tseng, X. Feng, M. Osada, E. Been, Y. Hikita, *et al.*, *preprint*, [arXiv:1909.02678](https://arxiv.org/abs/1909.02678) (2019).
- [70] M. W. Chase, *NIST-JANAF Thermochemical Tables* (J. Phys. Chem. Ref. Data, Monograph, 1998).
- [71] K. Haule, J. H. Shim, and G. Kotliar, *Phys. Rev. Lett.* **100**, 226402 (2008).
- [72] M. Aichhorn, L. Pourovskii, V. Vildosola, M. Ferrero, O. Parcollet, T. Miyake, A. Georges, and S. Biermann, *Phys. Rev. B* **80**, 085101 (2009).
- [73] V. I. Anisimov, D. M. Korotin, M. A. Korotin, A. V. Kozhevnikov, J. Kuneš, A. O. Shorikov, S. L. Skornyakov, and S. V. Streltsov, *Journal of Physics: Condensed Matter* **21**, 075602 (2009).
- [74] P. Hansmann, R. Arita, A. Toschi, S. Sakai, G. Sangiovanni, and K. Held, *Phys. Rev. Lett.* **104**, 197002 (2010).
- [75] A. Toschi, R. Arita, P. Hansmann, G. Sangiovanni, and K. Held, *Phys. Rev. B* **86**, 064411 (2012).
- [76] I. A. Nekrasov, N. S. Pavlov, and M. V. Sadovskii, *JETP Letters* **102**, 26 (2015).
- [77] D. Guterding, S. Backes, M. Tomi, H. O. Jeschke, and R. Valent, *physica status solidi (b)* **254**, 1600164 (2017).